

A Designing of Humanoid Robot Hands in Endo skeleton and Exoskeleton Styles

Ichiro Kawabuchi

*KAWABUCHI Mechanical Engineering Laboratory, Inc.
Japan*

This PDF is an author's copy.

Published in "Humanoid Robotics New Developments"
by Advanced Robotic Systems International in June 2007

1. Introduction

For a serious scientific interest or rather an amusing desire to be the creator like Pygmalion, human being has kept fascination to create something replicates ourselves as shown in lifelike statues and imaginative descriptions in fairy tales, long time from the ancient days. At the present day, eventually, they are coming out as humanoid robots and their brilliant futures are forecasted as follows. 1) Humanoid robot will take over boring recurrent jobs and dangerous tasks where some everyday tools and environments designed and optimised for human usage should be exploited without significant modifications. 2) Efforts of developing humanoid robot systems and components will lead some excellent inventions of engineering, product and service. 3) Humanoid robot will be a research tool by itself for simulation, implementation and examination of the human algorithm of motions, behaviours and cognitions with corporeality.

At the same time, I cannot help having some doubts about the future of the humanoid robot as extension of present development style. Our biological constitution is evolved properly to be made of bio-materials and actuated by muscles, and present humanoid robots, on the contrary, are bounded to be designed within conventional mechanical and electric elements prepared for industrial use such as electric motors, devices, metal and plastic parts. Such elements are vastly different in characteristics from the biological ones and are low in some significant properties: power/weight ratio, minuteness, flexibility, robustness with self-repairing, energy and economic efficiency and so on. So the "eternal differences" in function and appearance will remain between the human and the humanoid robots.

I guess there are chiefly two considerable ways for developing a preferable humanoid robot body. One is to promote in advance a development of artificial muscle that is exactly similar to the biological one. It may be obvious that an ideal humanoid robot body will be constructed by a scheme of putting a skeletal model core and attaching the perfect artificial muscles on it (Weghel et al., 2004, e.g.). Another is to establish some practical and realistic designing paradigms within extensional technology, in consideration of the limited performance of mechanical and electric elements. In this way, it will be the key point that making full use of flexible ideas of trimming and restructuring functions on a target. For example, that is to make up an alternative function by integrating some simple methods, when the target function is too complex to be a unitary package. Since it seems to take long time until the complete artificial muscles will come out, I regard the latter way is a good prospect to the near future rather than just a compromise.

In searching the appropriate designing paradigms for humanoid robots, it may be just the stage of digging and gathering many diverse and unique studies, styles and philosophies of the designing. After examining their practicability, reasonability and inevitability through the eyes of many persons over the long time, it will work out the optimised designing paradigms. I believe the most outstanding ingenuities in mechanical design are brought out in robot hands, as they are most complex mechanical systems on a humanoid robot body. Fortunately, I have had some experiences of designing them in each endoskeleton and exoskeleton styles. To contribute on such evolutive process as a mechanical engineer, I bring up here some of my ideas of designing robot hands.

2. Humanoid Robot Hand in Endoskeleton Style

2.1 Basic Design Conditions

There are two opposite orientations in planning specifications of a robot hand. One is emphasizing similarity in motion and function to the human hand. Another is emphasizing similarity in size and weight. A robot hand following the former orientation tends to become rather large against the human hand. Although attempts to make it small and light have been done by putting the actuators away into a forearm segment and actuating the fingers via links or wires (Jacobsen, 1984, e.g.), the whole system is still large and heavy as a load at an end of arm. A robot hand following the latter orientation tends to lack functions as shown in general prosthetic hands. Most research robot hands, except some modern prosthetic ones (Harada hand, e.g.), are designed following the former orientation to enlarge their universality on study scenes. And it is rational estimation that the properties aimed in the latter orientation will be resolved spontaneously as the industrial progress leads general mechanical and electric elements high-performance. However, I have taken the latter orientation, because I believe it should be also constitutive approach to an ideal robot hand, moreover it is challenging for me to contrive novel designs of complex mechanisms. Then I have set the basic design conditions as shown on Table 1.

1. Outline should be similar to the human hand with 5 fingers.
2. Every motor should be embedded within the outline, and connections with outside controller and power source are limited to some slim and limber electric cables.
3. Compactness and lightness should be equal to the average naked human hand. Concretely, mass is at most 500g, longitudinal length from fingertip to prospective center of wrist is at longest 200mm, and diameter of fingers is at most 20mm.
4. As far as the third condition is satisfied, number of motors and range of finger movements should be enriched for realizing some practical functions like holding bulk object, pinching thin card, and the most sign language. As key finger motions, all fingers move widely from opening to clenching, and the thumb and each of other fingers contact opposing on both fingertips.
5. As far as the fourth condition is satisfied, power of motors and robustness of mechanisms should be augmented. The desirable output force at each fingertip is over 5N under a straight posture.

Table 1. The basic design conditions.

2.2 Kinematical Arrangement of Joints

Fig. 1 shows the kinematical arrangement of joints in my robot hand. I identified each joint with two numbers and describe it as symbol $J_{n,m}$, in which the first suffix means finger number and the second one means joint number on each finger. The reason I avoid the popular joint nomenclature with the anatomical term like MP (metacarpal phalangeal joint) and DIP (distal interphalangeal joint) is that some of original human joints are complex one with multi degree of freedom (DOF) and hardly be substituted by a unitary joint mechanism.

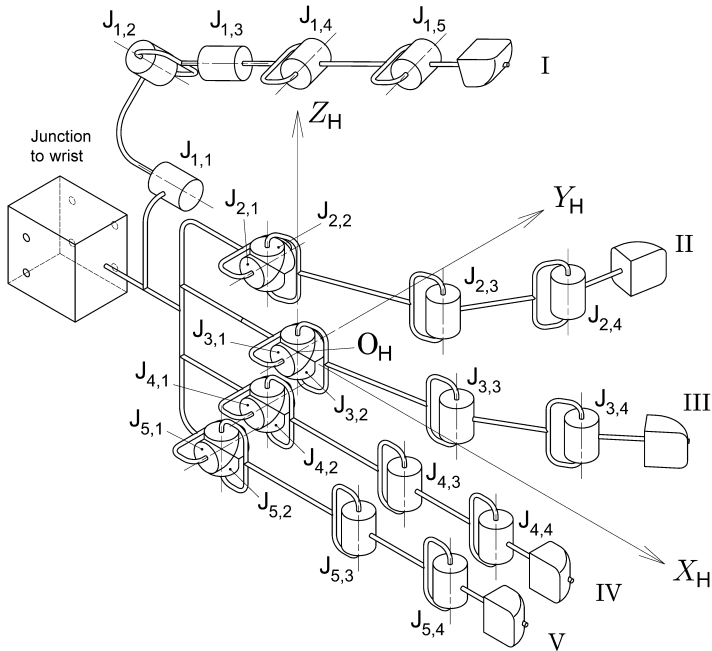


Fig. 1. The kinematical arrangement of joints.

The joint arrangement on the four fingers except the thumb would be common to most humanoid robot hand. At the same time, difference of thumb structures between several competitive robot hands (Fig. 2) shows clearly the diverse design philosophies following individual purposes and available technologies. The every thumb structure on Fig. 2 has a complex joint that consists of a pair of revolute joints intersecting their axes at one point. The complex joint is an influential technology and the Shadow hand, above all, has two ones to realize the most similar action and appearance to those of human. On the other hand, I avoided such joint with estimating its complexity will require large space that violates the basic design conditions when it would be designed by my present technical capabilities.

The order of each direction of joint axis and fingertip is also an influential characteristic for range and variety of the thumb motion. Especially in the NASA hand, to compensate disadvantages by low of DOF, the order is decided advisedly with considering a reasonable emulation of human thumb motion (Lovchik & Diftler, 1999). In my robot hand, the axis direction of joint $J_{1,3}$ is set for twisting the thumb tip that will conduce a stable pinching mentioned after. The axis directions of two joints $J_{1,1}$ and $J_{1,2}$ are decided mainly because of convenience to embed reducers with wide movable range.

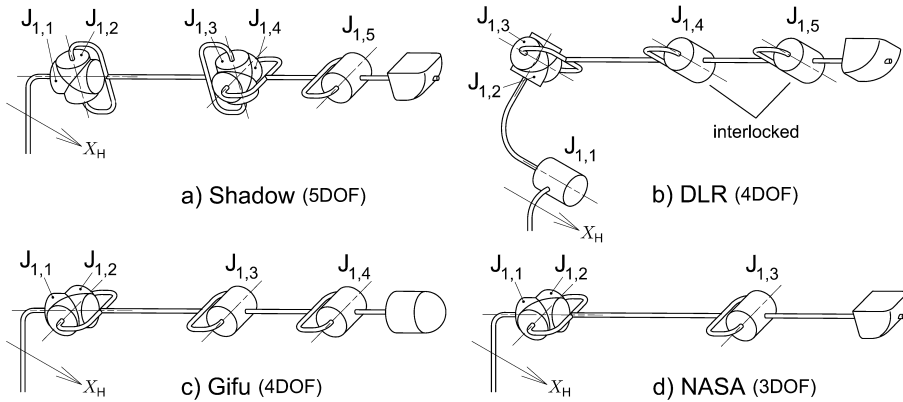


Fig. 2. Thumb structures of competitive robot hands.

2.3 Compression of Independent DOF

An “actuator assembly” that consists of a motor, an encoder and a reducer occupies considerable space in robot hand rigidly. Therefore, to plan a compact robot hand, it is a reasonable way to compress the number of equipped assemblies. This means furthermore compression of the independent DOF on the robot hand, so I pursued this idea boldly with keeping a reasonable emulation to the human hand motion.

In the four fingers except the thumb, most robot hands are designed with the two distal joints $J_{n,3}$ and $J_{n,4}$ coupled-driven by one motor, since those joints in the human hand often move together. I furthered this idea of interlocking and made all three joints $J_{n,2}$, $J_{n,3}$ and $J_{n,4}$ interlocked. In the same way, the relative opening-closing motion among the four fingers at the three root joints $J_{2,1}$, $J_{4,1}$ and $J_{5,1}$ is also interlocked. Moreover the joint $J_{3,1}$ is eliminated since the human middle finger rarely moves at the joint. In the thumb, the two distal joints $J_{1,4}$ and $J_{1,5}$ are interlocked and the joint $J_{1,3}$ is fixed in a certain angle.

Based on the consideration above, the essential independent DOF was extracted into 8. The member joints for each DOF are listed on Table 2(a) and named the “essential set”. Although the essential set can realize almost all required finger motions like making a loop with the thumb and the little finger, it lacks sophisticated dexterity for some delicate handlings like pinching a thin card. At last, I have added some DOF on the essential set as listed on the Table 2(b) and it is named the “latest set”.

In the following two sections I explain mechanisms corresponding to the essential set, and in the later sections I introduce more complex mechanisms corresponding to the latest set.

Member	Member
1 $J_{1,1}$	5 $J_{2,2}+J_{2,3}+J_{2,4}$
2 $J_{1,2}$	6 $J_{3,2}+J_{3,3}+J_{3,4}$
3 $J_{1,4}+J_{1,5}$	7 $J_{4,2}+J_{4,3}+J_{4,4}$
4 $J_{2,1}+J_{4,1}+J_{5,1}$	8 $J_{5,2}+J_{5,3}+J_{5,4}$

(a) The essential set (8DOF)

Member	Member	Member
1 $J_{1,1}$	6 $J_{2,1}+J_{4,1}+J_{5,1}$	11 $J_{3,4}$
2 $J_{1,2}$	7 $J_{2,2}$ (differential)	12 $J_{4,2}+J_{4,3}$
3 $J_{1,3}$	8 $J_{2,2}+J_{2,3}$	13 $J_{4,4}$
4 $J_{1,4}$	9 $J_{2,4}$	14 $J_{5,2}+J_{5,3}$
5 $J_{1,5}$	10 $J_{3,2}+J_{3,3}$	15 $J_{5,4}$

(b) The latest set (15DOF)

Table 2. The independent DOF set and member joints.

2.4 Global Finger Flexion Mechanism

As mentioned in the section 2.2 a complex joint in which two rotational axes intersect was avoided in the thumb mechanism, however, the other four fingers retain such complex joint at the root. The difficulties in developing such complex joint include how electric wirings are passed through the joint. The delicate wirings should not be overstretched due to joint rotation, so the wirings should be passed just or near the intersection point of two axes. I introduced a scheme that no part of an actuator assembly is placed around the intersection but enough empty space only for the wirings, at the same time the rotational power for the two axes is provided via wire or link mechanism from an off-site motors.

Fig. 3 shows the internal structure of a basic finger, all the four fingers have the same mechanism. A small DC motor with a built-in encoder (Faulhaber, model 1516SR or 1319SR) is embedded in the largest finger segment lengthwise, like filling the segment volume. A reducer that consists of a crown gear train and two-stage planetary gear train is built in the joint $J_{n,3}$ and drives it. For optimum integration: a combination of larger and smaller gears is effective in uniting higher reduction ratio and efficiency, axes of all gear trains are arranged coaxial to that of joint $J_{n,3}$, so that volume of the joint part admits possibly largest diameter of gears without making the finger segment longer. In the actual reducer, the crown gear which diameter is almost equal to that of finger segment engages with the motor pinion and derives 10 times torque efficiently. In a general gear train with axes mutually orthogonal, the rigidity is low and the play is generated easily; so it is reasonable putting the crown gear train at the first stage viewed from the motor, where the transmission torque is low and the influence of play is negligible. Moreover the planetary gear train is constructed as a unique mixture of planetary-type and star-type for most compactness, so this reducer gets high reduction ratio 1/350 and the maximum joint torque is at least 0.5Nm.

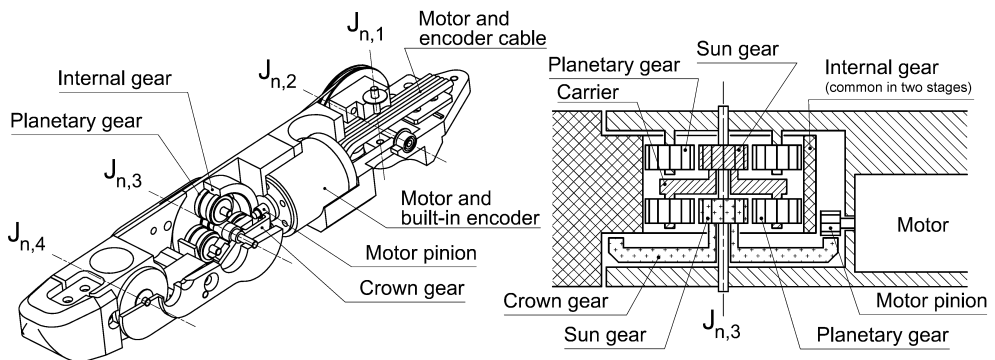


Fig. 3. The internal structure of a basic finger.

It is very important feature of a robot hand that it has smooth back-drivability at each joint for stable control of contacting force on a fingertip. I think it is more acceptable a slight play at gears as a consequence of high back-drivability than a large frictional resistance of gears as a consequence of elimination of the play, thanks to the general robot hand is demanded to perform relatively small force and low absolute accuracy in finger motions. So the actual fingers of my robot hand are manufactured with slight play to get most back-drivability; each finger can be moved passively by small force on the fingertip at most about 0.3N.

The interlocking mechanism among the three joints $J_{n,2}$, $J_{n,3}$ and $J_{n,4}$ consists of wire-pulley mechanisms with pulleys carved on the sidewall (Fig. 4(a)). Since they are thin enough the finger segments afford some internal space for motor, sensor and electric component. Although identical transmission can be constructed using a link mechanism, it tends to become larger due to restriction on facilitating smooth transmission in large rotational angle near 90degree. Considering a reasonable emulation of the human motion, the transmission ratios are set 7/10 from $J_{n,3}$ to $J_{n,2}$, and 5/7 from $J_{n,3}$ to $J_{n,4}$ respectively (same (b)).

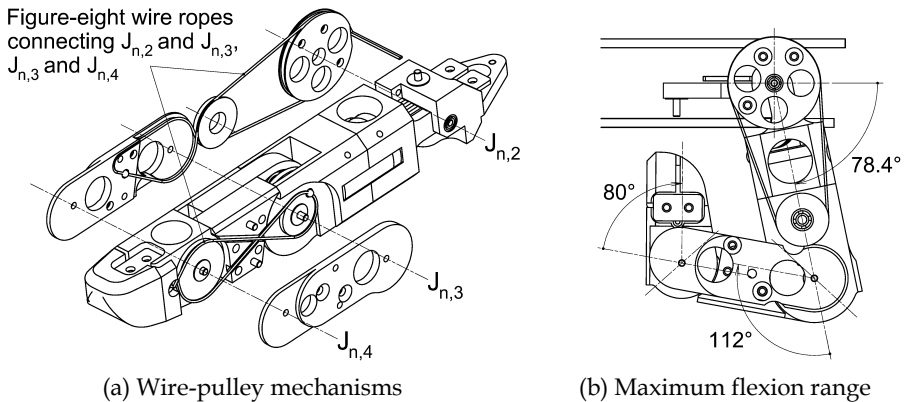


Fig. 4. Interlocking mechanism of the global finger flexion.

2.5 Abduction-Adduction Mechanism

Since the relative opening-closing motion among the four fingers except the thumb is called abduction-adduction in the anatomical term, the interlocking mechanism among the three joints $J_{2,1}$, $J_{4,1}$ and $J_{5,1}$ was named after it. Introduction of this mechanism has mainly two reasons as follows. The first is cutting back on the actuator assembly. The second is a practical idea that the ring and little fingers do not need such motion independently, because they on the human hand rarely take part in a dexterous pinching function. So it can be said that the target of this mechanism is only generating a relative opening-closing motion between the index finger and the middle finger.

Rotational angle of those joints is small, so this mechanism is constructed as a link mechanism (Fig. 5), and in quest of efficiency and compactness it is designed as below. The joint $J_{4,1}$ is selected as driven by a motor directly, so that the power transmission to other joints becomes the shortest route with high efficiency and low adverse influences like play. To obtain a large gear ratio with possibly least stages of gear train, a large sector gear that passes over the palm longitudinal length is adopted and fixed on the joint $J_{4,1}$ (Fig. 6(a)), and the entire reduction ratio is implemented as 1/400. Thanks to the drive motor is located on the edge of the palm, over half of the space in the palm can be free for electric components. Even when each finger is bent to the maximum flexion as shown in the Fig. 4(b), the opening-closing motion can act independently thanks to the clearance between fingertip and palm; the robot hand can perform V-sign actions, e.g. freely. An electric printed circuit board (PCB) that contains a microcomputer for local processing, motor amplifiers, motor current sensors and an interface unit communicating with an outside controller through a serial signal line, is embedded like filling almost all the space in the palm (Fig. 6(b)).

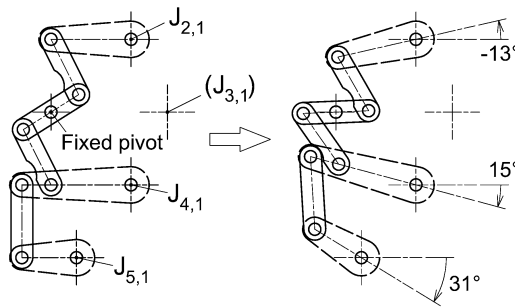
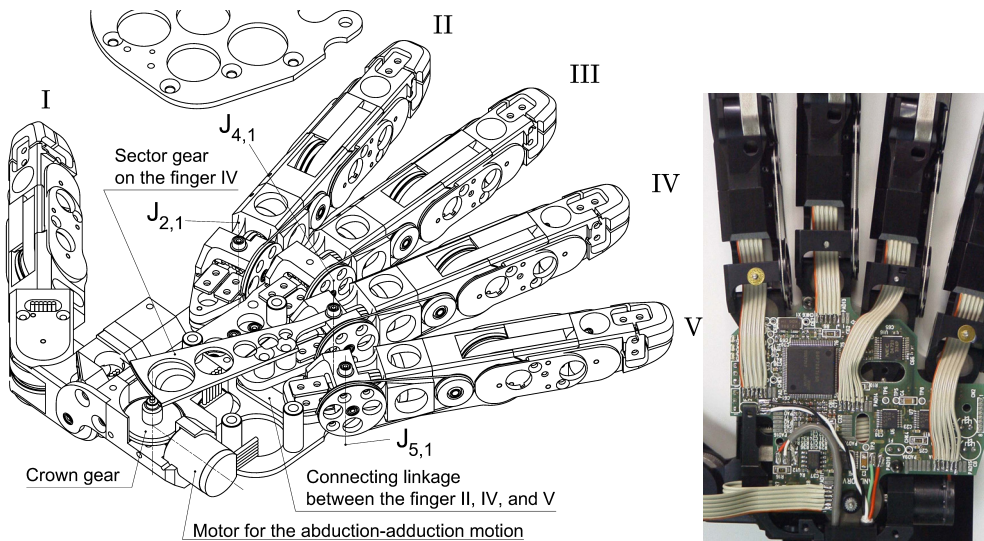


Fig. 5. Connecting linkage for the abduction-adduction motion.



(a) Location of the reduction gears and the linkage
 Fig. 6. Mechanism and electric equipment in the palm.

(b) Embedded PCB

2.6 Introduction of Independent Fingertip Motion

Stably and softly pinching thin paper and handling small piece in complicated shape are the vital functions for a humanoid robot hand, when it could be recognised dexterous enough. To realize these delicate functions, the key feature is a fine force and motion control on the fingertips. The human finger has excellent feature of controlling them finely in any direction, and furthermore it can generate large force in case of necessity. On the contrary, usual small actuator assembly that consists of motor and geared power train never has such large “dynamic range” in force control. In case of my robot finger, the main actuator assembly for the global finger flexion should be designed to generate possibly larger force for moving itself in sufficient speed against its mass and inertia, and moreover grasping a heavy object. Then it is hard for the actuator to be expected to generate fine force on the fingertip.

2.7 Independent Terminal Joint Mechanism

The mechanical feature necessary for the new handling strategy above is a smooth compliance of fingertip to an object, in concrete terms a following motion to keep a soft contacting force. Although a similar feature could be produced with adding a spring on the way of power transmission to the fingertip, the spring occupies not negligible space in the small finger segment. Another way introducing a force sensor on the fingertip is also hard in acquiring appropriate sensor and tuning up a force feedback controller robust. So the most practical way to realize the compliance is exploiting a simple open-loop torque control method of the motor only by observing its current.

In this case, it requires a high efficient reducer with low frictional resistance and play of gears. I adopted a gear train that uses only high precision spur gears with expectation of their high efficiency. The motor length is restricted to the width of the finger segment, because the motor must be laid widthwise to be parallel to the joint axis. I searched on the web a possibly higher performance motor that fits into the limited length, and found a small DC motor (Sanyo Precision, model KS-2717) in production for small electric appliances. Since the output torque of the motor is very small 0.5Nmm in maximum, the reduction ratio is needed to be possibly higher. To realize high gear ratio avoiding deterioration of efficiency and inflation of volume, a two-stage thin gear train is built in against a sidewall with combining possibly largest and smallest gears for maximizing the gear ratio (Fig. 8); the gear module is 0.16 and the number of smallest gear's teeth is only nine. Consequently, the gear ratio is 3/250, and the maximum fingertip force is almost 2N.

A thin potentiometer is introduced to measure the angular displacement and put against another sidewall. By this alignment of the reducer and the potentiometer on the both sidewalls, the finger segment retains enough empty space inside.

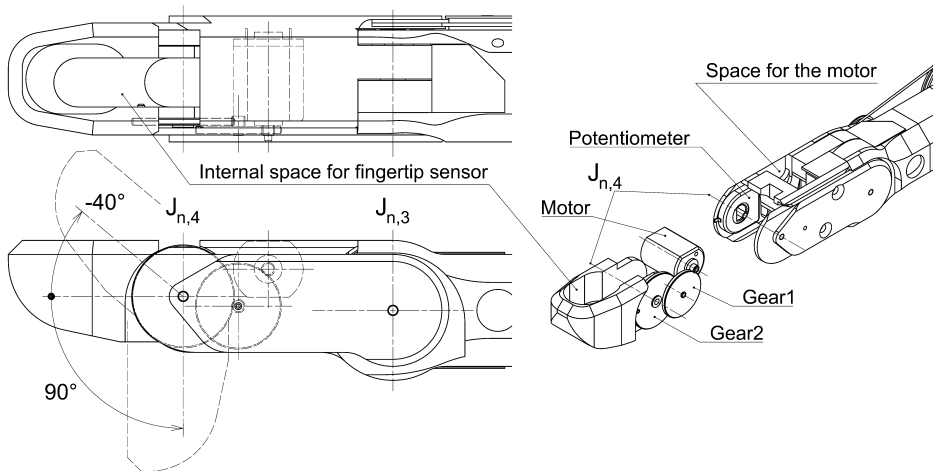


Fig. 8. Actuator assembly for the independent terminal joint.

To confirm the smooth compliance of a fingertip, a primary experiment was conducted. Concretely I examined active spring effect of the joint $J_{n,4}$ generated as follows. The joint $J_{n,4}$ was always position-controlled to keep its angular displacement $\theta_{n,4}$ at a certain target. The original target was set 0, that meant the terminal segment and middle segment were in line.

When the motor current of the joint $J_{n,4}$ exceeded a certain threshold, the target was shifted gradually to a temporary target by adding/subtracting a small variation proportional to the difference between the threshold and the present motor currents, so that the excess of motor current got reduced. When the motor current fell below the threshold and besides the temporary target was different from the original one, the temporary target was restored gradually to the original one by adding/subtracting a small variation proportional to the difference between the latest temporary target and the original one. In consequence of repeating this control in high frequency, the active spring effect was created stably.

In the experiment, the external pressure for examining the compliance was provided by the other finger part. Concretely, the finger part between the joints $J_{n,2}$ to $J_{n,4}$ was moved repeating a slight sine wave motion by a position-control of the main motor, and kept pressing the fingertip against a fixed object. Contacting force between the fingertip and the object was measured using a film-like force sensor (Nitta, FlexiForce) placed on the object; as a matter of course the observed force was not used in the motor control.

Fig. 9 shows the result of experiment with transitions of the contacting force and the angular displacement $\theta_{n,4}$. The threshold of motor current was set in two values as examples that provide the limits of contacting force as about 0.9N and 1.4N respectively. Effectiveness of the smooth compliance of fingertip is confirmed by analysing each transition as follows. When the contacting force just exceeded the limit, the joint $J_{n,4}$ started to rotate to release the excess, so that the contacting force was stuck at the limit. The joint $J_{n,4}$ started to return to the original position when the contacting force fell below the limit. These movements are just the characteristics of desirable compliance. And stable constancy of the maximum contacting force at the limit reveals high efficiency of force transmission through the reducer, and prove adequacy of the estimating way of contacting force from the motor current. This smooth compliance cannot be produced by a simple spring mechanism because it cannot change the output force freely, then this practical function with minimum additional parts is one of the distinctive features on my robot hand.

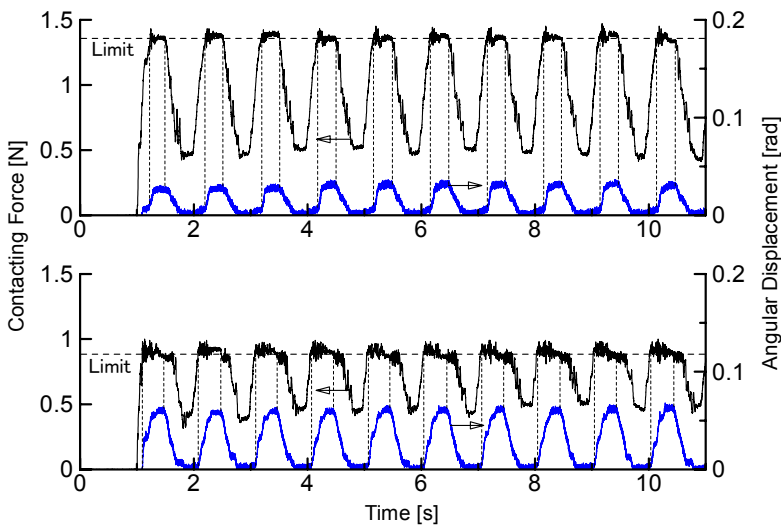


Fig.9. Experimental result of the contacting force and the angular displacement of a fingertip.

2.8 Thumb Twisting Mechanism

To fully maximize the capability of the smooth compliance generated by the independent terminal joint mechanism, the direction of fingertip force should be oriented rightly in the normal line of contacting surface on an object. This manner furthermore increases the stability of pinching in pressing the surface by entire flat pad on the fingertip. In order to realize this manner concretely, either or both of cooperating fingers in a pinching need to twist its fingertip along its longitudinal axis in a considerable angular displacement. Then I gave the thumb the distinctive joint $J_{1,3}$ for this twisting function.

Fig. 10(a) shows 5 segments in the thumb; each segment is identified with the number starting from the root, and described as symbol $S_{1,n}$. In the primitive robot hand with the essential 8DOF, the two segments $S_{1,2}$ and $S_{1,3}$ are integrated by fixing the twist angle. Avoiding deterioration of the original mechanical harmony, the actuator assembly for the joint $J_{1,3}$ was designed additionally. To minimize the joint $J_{1,3}$ volume, cylindrical case of the motor for the joint $J_{1,4}$ that is already embedded over segments $S_{1,2}$ and $S_{1,3}$ is exploited as the axis of $J_{1,3}$. Unlike the terminal joint mechanism, this twist function requires relatively large motor for moving large mass of the finger structure, so a bulge is added on the segment $S_{1,2}$ to mount a motor same as that for the global finger flexion (Fig. 10(b)). Although this bulge is a little unbecoming, I accept it as a reasonable way for preventing stretch of the thumb length. The movable range of twisting is 45degree.

By the way, the two joints $J_{1,1}$ and $J_{1,2}$ have the same actuator assembly for the global finger flexion shown in the Fig. 3, and each has adequate movable range of over 120degree and 60degree respectively.

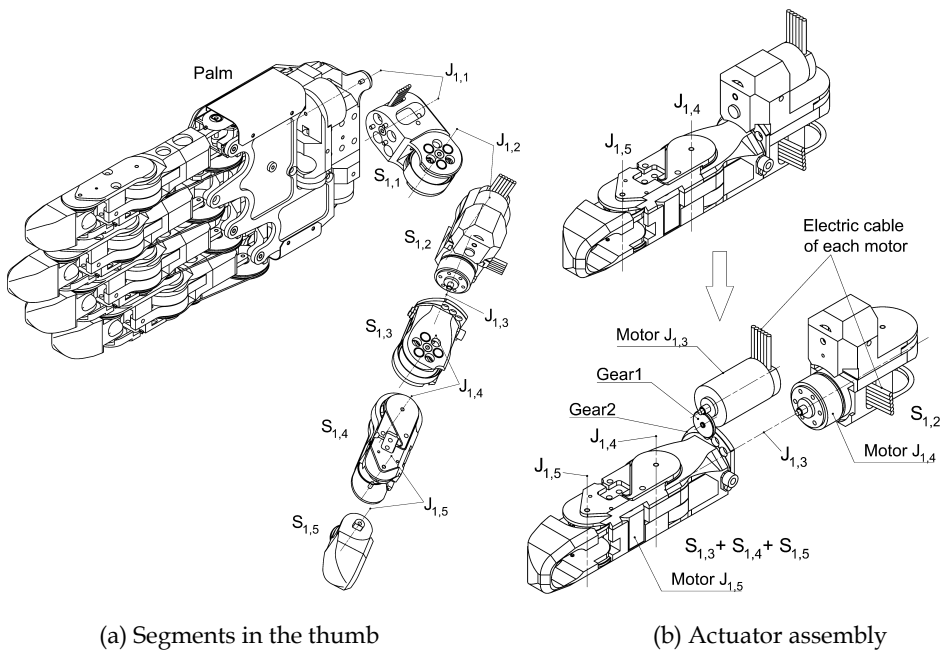


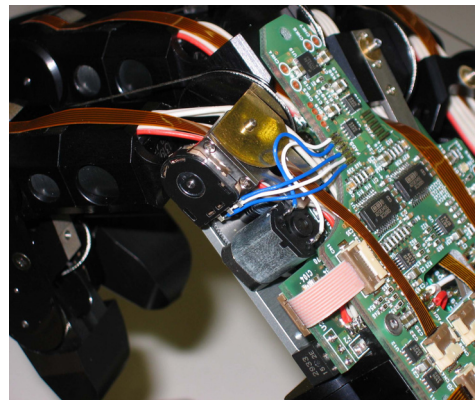
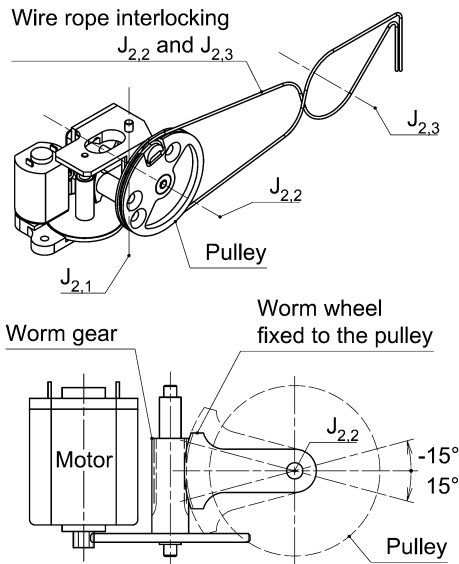
Fig. 10. Thumb mechanism with twisting function.

2.9 Independent Root Joint Mechanism

In the four fingers except the thumb, since the both joints $J_{n,2}$ and $J_{n,3}$ need no little power in the global finger flexion, the idea of interlocking these two joints and actuating them by one relatively large motor has adequate rationality, as far as the finger has no more capacity to accept two motors for actuating them independently. However, in some cases, the independent motion of each joint is required to realize some slight motion like adjusting the contacting place of a fingertip on an object. In order to demonstrate my technical capability to realize such complex requirement additionally, an actuator assembly was introduced at the joint $J_{2,2}$ particularly.

As a matter of course there is no capacity to accept a large motor, the additional motor is selected as the same small one driving the terminal joint. As the global finger flexion should be generated by the existing mechanism, the additional small actuator assembly should be designed to generate a differential motion as being overlapped on the global finger flexion. Well, the pulley on the joint $J_{2,2}$ is existing as a basement of the global finger flexion and its shape is round and coaxial to the axis of joint $J_{2,2}$, so it is convenient for realizing the differential motion by rotating the pulley around the axis.

Fig. 11 shows the actuator assembly to rotate the pulley. To sustain the large torque around the joint $J_{2,2}$ for the global finger flexion, it needs possibly larger reduction ratio. Therefore a worm gear train, that generally has large gear ratio, is introduced, so that the entire reduction ratio gets 1/1000. Although a worm gear train has no back-drivability, it is also an advantage in this case because that gear train can support any large torque in case of necessity. The movable range of the pulley is $+15^\circ$ to -15° that makes useful adjusting motion at the fingertip in 10mm order.



(a) Worm gear mechanism to drive the pulley

(b) Actual embedded situation

Fig. 11. Differential mechanism for the independent root joint motion.

2.10 Smart Wiring for Bypassing Reducer

The quality of a robot system is evaluated from many kinds of dimension including neatness of the electric wiring, since its weight and volume can bring recognizable deterioration in the performance of high-speed motion and indisputably deteriorate the appearance. The lack of space for containing the wiring is the most common cause of this problem because expelling the wiring outside makes its weight and volume to increase. In my robot hand, as mentioned in the section 2.4, the discussion about the designing root joint structure of each finger was started by consideration of this problem. And more problem is outstanding around the joint filled with the large reducer of ratio 1/350 meaning $J_{1,1}$, $J_{1,2}$, $J_{1,4}$, $J_{2,3}$, $J_{3,3}$, $J_{4,3}$ and $J_{5,3}$. Recognizing the significance of this problem, a unique and practical design of wiring is introduced.

The role of the wiring is electric connection between the motor and sensor for the terminal joint and the main PCB in the palm, and a thin flexible PCB with 3.5mm width makes it. When the wiring is led as going around the reducer's circular outline, the change of shortest path length due to the finger flexion is remarkable, and then the method to retract and extract the corresponding length of wiring becomes the practical problem. My robot hand, fortunately, has enough margin space in the finger segments, and it can be formed an empty space where the wiring can adapt to the change of path length with changing the curving line by itself as shown in Fig. 12.

By the way, this wiring style cannot be adopted on the two thumb root joints $J_{1,1}$ and $J_{1,2}$ because of lack of the internal space, and then the wirings through these joints are forced to go outside in a wide circle unbecomingly. This problem will be solved in the next development step waiting for an investment opportunity.

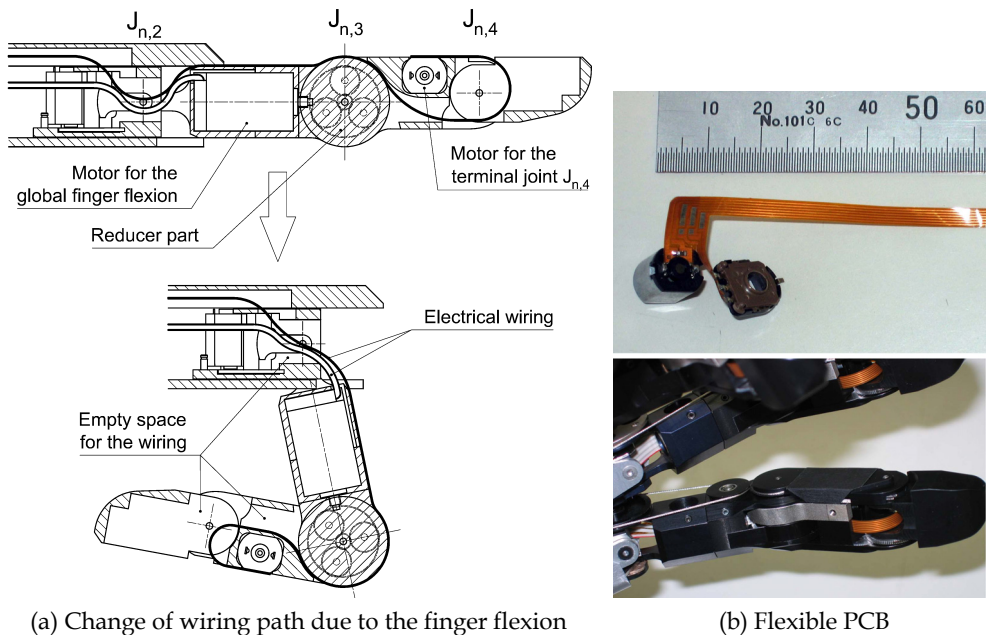


Fig. 12. Design of the wiring around the joint that contains the large reducer.

2.11 Overall view of the Humanoid Robot Hand

As a conclusion of all previous considerations the latest model of my robot hand is built up as shown in Fig. 13; it has 15DOF as defined on the Table 2(b) while it satisfies the basic design conditions on the Table 1. The total mass including the internal electric equipment except the long cable connecting outside controllers is just 500g. The connections to outside systems are only $\phi 2.4$ signal cable and $\phi 4.5$ power cable. Some dimensions of details like the length of each finger segment are referred to my hand.

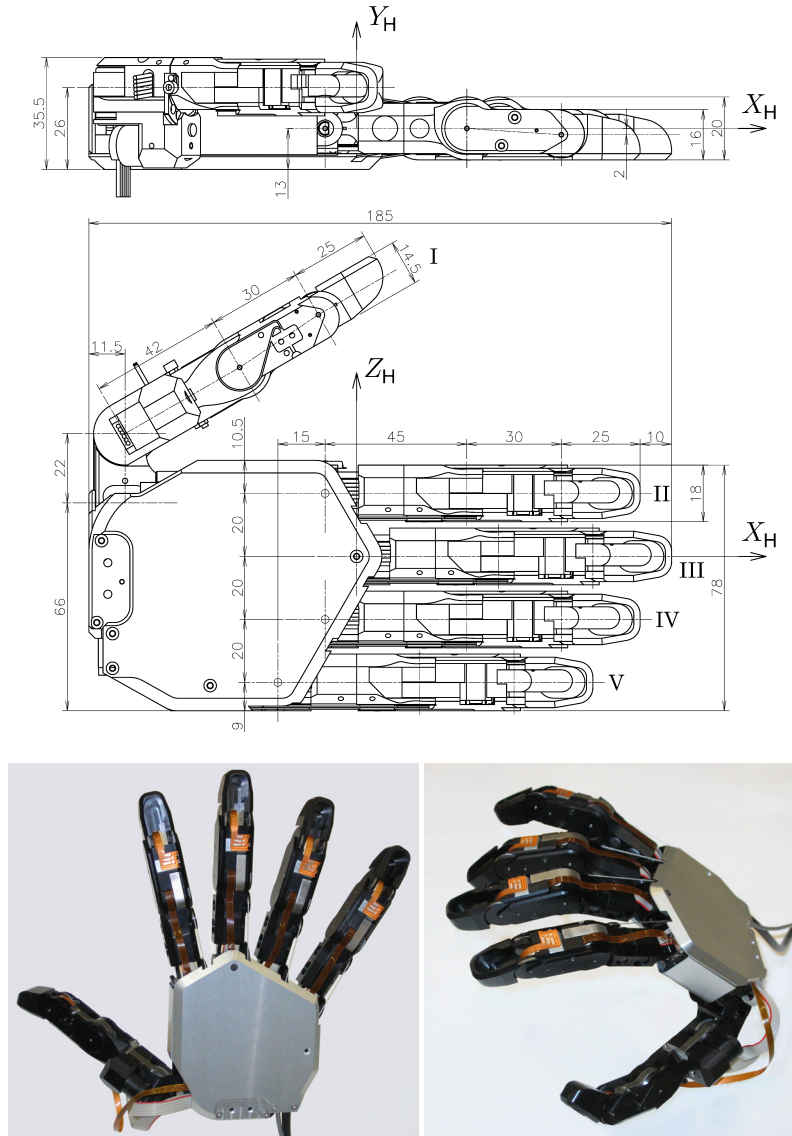


Fig. 13 Overall profile of the latest model.

To confirm dexterity of the robot hand, some experiments of representative and practical handling motions were conducted; this paper displays two handling types: pinching a business card and holding a pen (Fig. 14). The key evaluation items in these experiments were the two distinctive functions: the smooth compliance on a fingertip and the twisting of the thumb. All the fingertip forces were generated by the simple open-loop torque control method explained in the section 2.7 without force sensors.

By the way, the smart wiring style explained in the section 2.10 is installed only to the latest model, and the robot hand used in the experiments did not have it unfortunately.

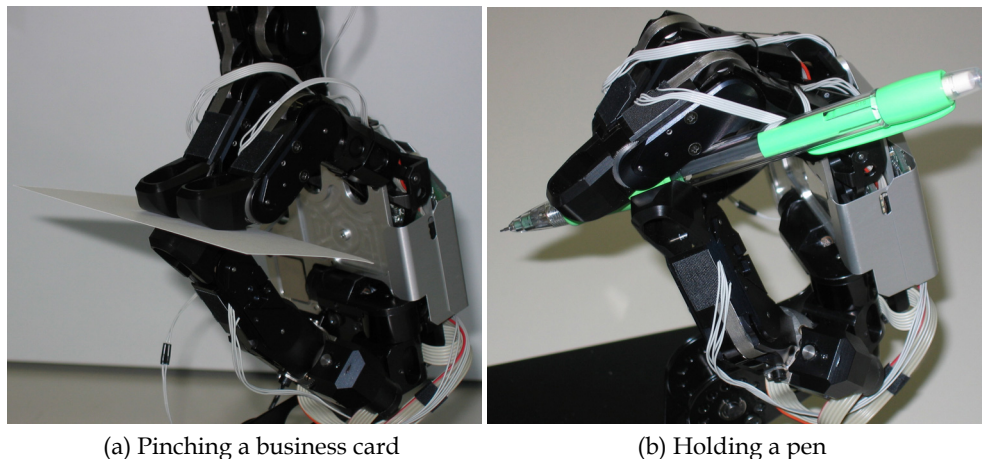


Fig. 14 The representative and practical handling motions.

In the experiment of pinching a business card, the robot hand performed switching several times two couples of pinching fingers: the thumb and the index finger/the thumb and the middle finger (Fig. 15). In the junction phase when all the three fingers contacted on the card, the thumb slid its fingertip under the card from a position opposing a fingertip to another position opposing another fingertip. In the experiment of holding a pen, the robot hand moved the pen nib up and down and sled the thumb fingertip along the side of the pen (Fig. 16). In both experiments, the objects: card and pen were held stably, and these achievements prove the contacting force appropriate in both strength and direction could be generated at each fingertip.

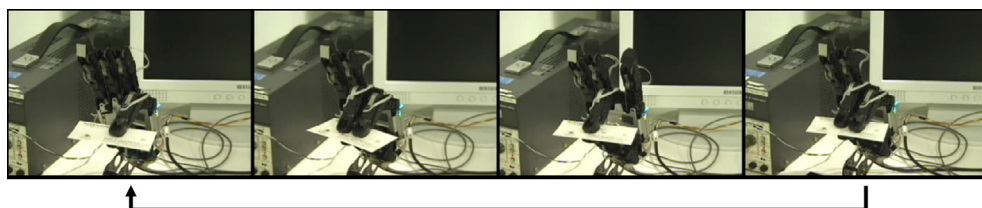


Fig. 15 Cyclical steps in the experiment of pinching a business card.

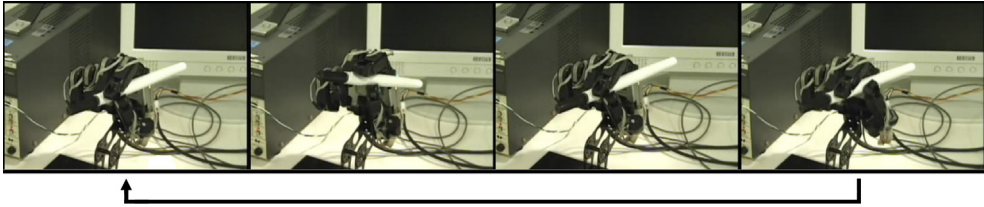


Fig. 16 Cyclical steps in the experiment of holding a pen.

At the SIGGRAPH 2006, I got an opportunity to join into a participating party of the “Hoshino K. laboratory in the university of Tsukuba” which introduced my humanoid robot hand for the first time. The robot hand was demonstrated on a humanoid robot arm that is actuated by pneumatic power, and has 7DOF wide movable range, slender structure and dimensions like an endoskeleton of a human arm (Fig. 17). While its power is low and the practical payload at the wrist joint is about 1kg, it could move the robot hand smoothly. The conclusive advantage of the robot hand is that many complex functions are condensed in the humanlike size, weight and appearance, and realize the sophisticated dexterity. As the robot hand has rich suitability for delicate robot arms, after more sophistication, it will be developed to a good prosthetic hand in the near future.

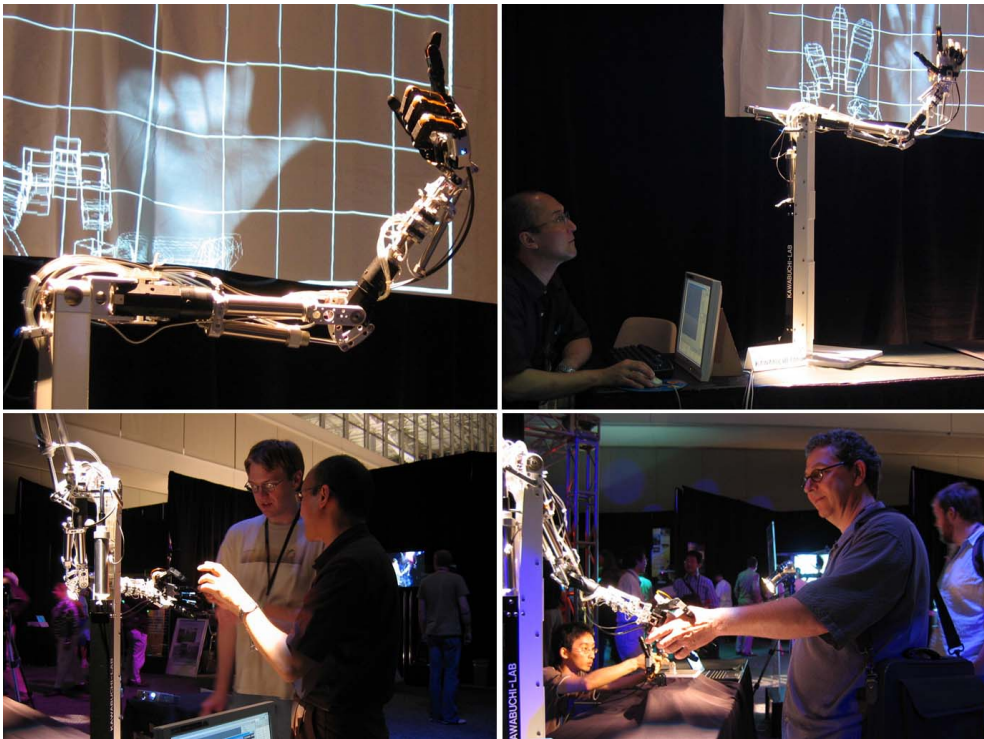


Fig. 17 Demonstration in the international exhibition SIGGRAPH 2006 in Boston.

3. Master Hand in Exoskeleton Style

3.1 Introduction of Circuitous Joint

As a dream-inspiring usage, the dexterous humanoid robot hand will be employed into a super “magic hand” with which an operator can manipulate objects freely from far away and get feedback of handling force and tactile sensations. Such intuitive master-slave control method of a humanoid robot with feedback of multi-modal perceptions is widely known as the Telexistence/Telepresence, however, developments of adequate master controllers for them have been rare in comparison with slave humanoid robots. I guess one of major reasons is a difficult restriction in mechanical design that any mechanism cannot interfere operator’s body. To solve this problem an idea of exoskeleton is brought up by association of a suit of armour that can follow wide movable range of human body with covering it.

The most popular and practical master hand in exoskeleton style is the CyberGrasp, and most conventional master hands in exoskeleton style have the similar structure to it. They are designed to be lighter and slenderer with less material, so they have no core structure and cannot sustain their form as a hand without parasitism on operator’s hand. This means they gives some constriction feeling to the operator and the slight force sensation in the feedback is masked. Then I have tried to design an ideal exoskeleton that fulfils every of lightness, slenderness and self-sustainability in its form.

In designing such exoskeleton, the main theme is focused on joint mechanisms. The most practical joint is a revolute one that consists of an axis and bearings, and general ways to place it corresponding to an operator’s joint are in parallel on backside or in coaxial beside. However, the former tends to deteriorate the movable range of operator’s joint (Fig. 18(a)) and the latter cannot find an existing space between operator’s fingers. Therefore I propose a novel joint mechanism named “circuitous joint” that has a virtual axis coincided with the axis of operator’s skeleton while the all mechanism exists on backside of operator’s finger. Technically this virtual axis is the instantaneous center of relative rotation of two segments. Fig. 18(b) shows the principle of the circuitous joint that realizes the virtual axis by stretching displacement s of two segments in proportion to the joint angular displacement θ .

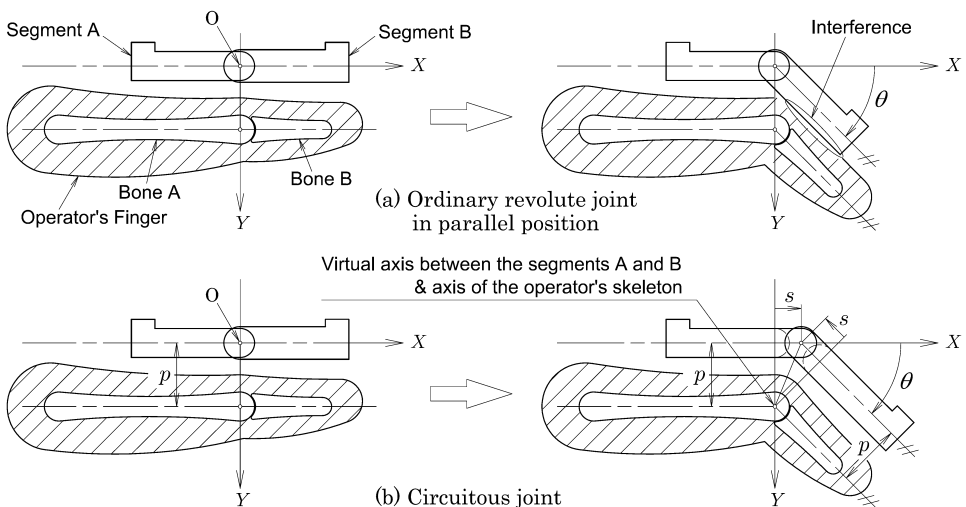


Fig. 18 Behaviour of two types of revolute joint in following operator’s finger.

3.2 Fundamental Mechanism of the Circuitous Joint

In order to realize the principle of the circuitous joint mentioned above, rack and gearwheel mechanism was adopted in consideration of high rigidity of structure, certainty of motion, and facility of manufacturing. Fig. 19 shows the fundamental mechanism prepared for a principle study. A gearwheel is rotated on a rack by relative rotation of two segments, and shifting of its axis provides stretching of a segment that has the rack (Fig. 20). Since the two segments should make same stretching displacement together, two sets of the mechanism are combined in opposite direction. The gearwheel is formed to be sector gear by removing unnecessary part. We may note, in passing, this mechanism is an “over-constrained” mechanism, so it can keep its behaviour even without the actual axis.

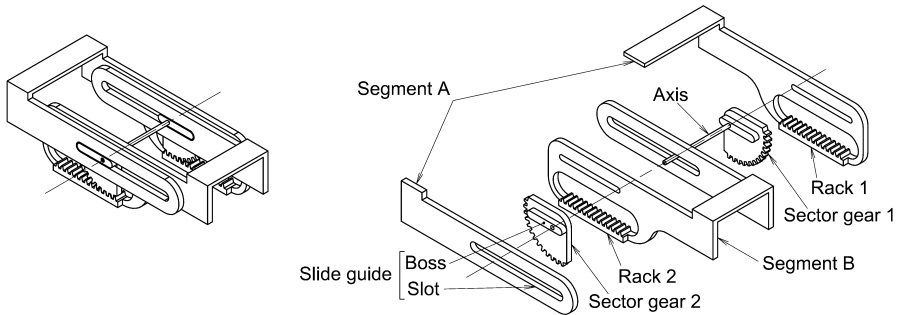


Fig. 19 The fundamental mechanism as a unit of the circuitous joint.

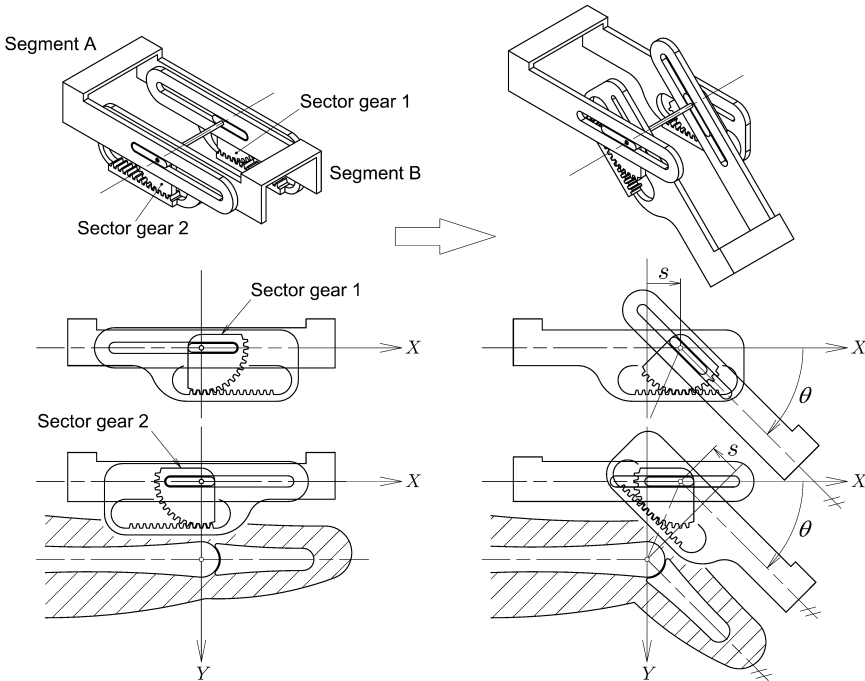


Fig. 20 Mixed motion of rotating and stretching of two segments.

3.3 Kinematical Design of the Optimal Circuitous Joint

To make the virtual axis coincide exactly to the axis of operator’s skeleton, the relationship between the angular displacement θ and the stretching displacement s must be non-linear. This means the rectilinear rack and the circular gearwheels should not be adopted, however, they can get practical use with optimal specifications calculated as follows.

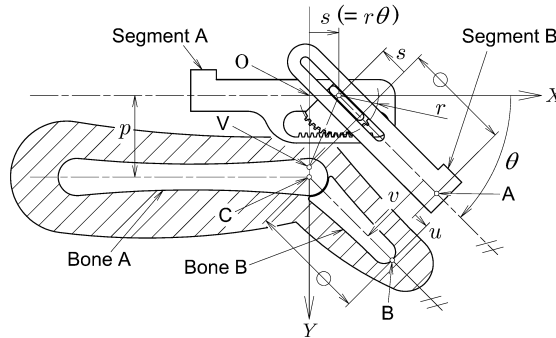


Fig. 21 Kinematical symbols in the circuitous joint.

Fig. 21 shows definition of kinematical symbols of parts and parameters; for example, point V is the virtual axis. The specifications that provide the shape of rack and sector gear are only the pitch circle radius r of the sector gear and the standard offset p between the center-lines of the Segment A and the Bone A. Since the standard offset p is decided 10mm due to convenience of practical design of mechanism, only the radius r is an object to be optimised. The point V moves on the Y-axis by change of θ and its behaviour is divided into three types according to the size of r (Fig. 22). Considering its nearest trajectory to the point C, the preferable range of r is presumed as $0.5p \leq r \leq (2/\pi)p$.

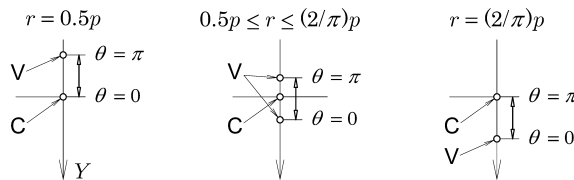


Fig. 22 Motion of the virtual axis V on the Y-axis by change of θ .

The evaluation item for the optimisation was set a deviation d defined by next formula that means deformation of kinematical relationship between two datum points A and B as shown in the Fig. 21, and the optimal radius r should minimise it.

$$d = \sqrt{u^2 + (p - v)^2} \quad \{ \text{where } u = -r\theta \cos\theta + p \sin\theta - r\theta, v = p \cos\theta + r\theta \sin\theta \} \quad (1)$$

Fig. 23 shows curves of the deviation d vs. θ in several settings of the radius r . The radius r is set within the presumed range. To generalise the optimisation each parameter is dealt as dimensionless number by dividing with the offset p . Screening many curves and seeking a curve which peak of d during a movable range of θ is minimum among them, the optimal r

is found as the value that makes the sought curve. For example, when the movable range is $0 \leq \theta \leq \pi/2$ the optimal radius r is $0.593p$ and the peak deviation d is $0.095p$, and when the movable range is $0 \leq \theta \leq \pi/3$ the optimal radius r is $0.537p$ and the peak deviation d is $0.029p$. As the offset p is set 10mm, the peak of d is below acceptable 1mm; therefore, the mechanism with rectilinear rack and circular gearwheels has practicability enough.

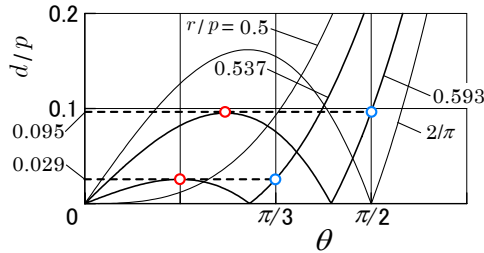


Fig. 23 Variation of curves of the deviation d .

3.4 Driving Method of the Circuitous Joint

To design the joint mechanism light and slender, a method to drive it from away via a wire rope is introduced. The wire rope is set along two segments veering by a pulley on the sector gear's axis, and one end is fixed on a segment and another end is retracted/extracted by a winding drum set at a stationary root (Fig. 24(a)). Since the wire rope can generate only pulling force that rotates the joint in straightening direction, a spring is added to generate pushing force that rotates it in bending direction (same (b)). This driving method has further conveniences to be applied to a tandem connection model (same (c)). A wire rope to a distal joint from the root can be extended easily through other joints. Its tensile force shares accessorially a part of driving force of other joints they are nearer to the root and need stronger driving force. Moreover, a coupled-driving method of plural joints can be realized only by winding their wire ropes together with one drum. The rate of each rotation can be assigned separately by independent radii on the drum.

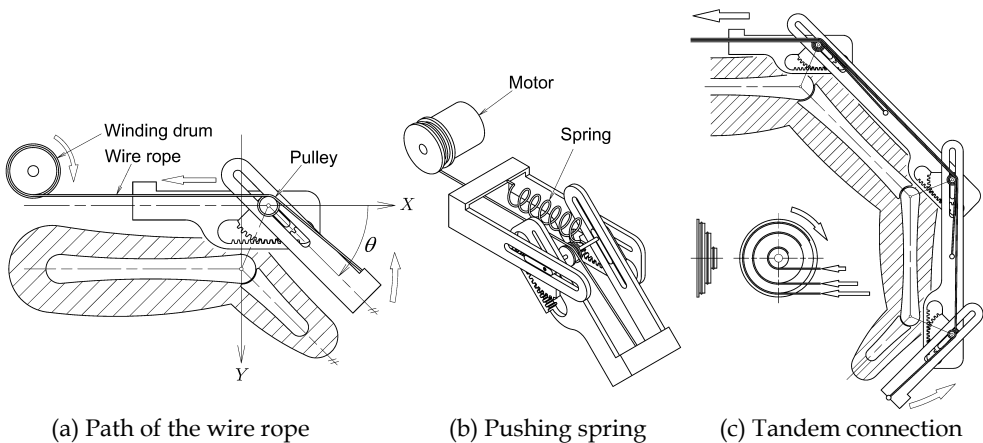
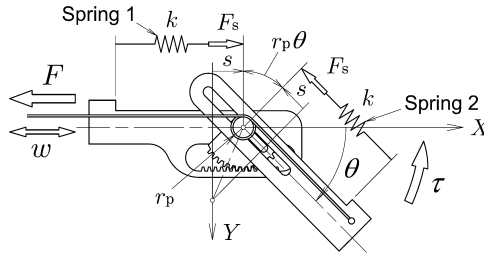


Fig.24 Driving method of the circuitous joint.



- r_p : Radius of the pulley (constant)
- k : Spring constant of the compression spring (constant)
- F_s : Spring force generated by the spring (intermediate variable)
- F_s' : Spring force generated by the spring when $\theta = 0$ (constant)
- w : Retracting/extracting displacement of the wire rope (input variable)
- F : Pulling force of the wire rope (input variable)
- θ : Joint angular displacement (output variable)
- τ : Joint torque (output variable)

Fig. 25 Statical symbols in the circuitous joint.

The definition of statical symbols is shown in Fig. 25, and the formulas for inverse statics calculating the input (manipulated) variables: w and F , from the output (controlled) variables: θ and τ are derived as follows.

$$w = (2r + r_p)\theta \tag{2}$$

$$F = \frac{1}{2r + r_p} \tau - \frac{2k \cdot r^2}{2(2r + r_p)} \theta + \frac{2F_s' \cdot r}{2r + r_p} \tag{3}$$

As these formulas show simple and linear relationship between the input and output valuables, this driving method promises further advantage that the algorithm of controlling both position and force is fairly simple. When the spring effect is negligible, as the second and third terms on the right side of formula (3) are eliminated, we would be able to control the output torque τ by using only the motor torque as the controlled variable.

3.5 Master Finger Mechanism (MAF)

Fig. 26 shows the practical master finger mechanism (MAF hereafter) corresponding to a middle finger of my hand and my humanoid robot hand, and proves the mechanism can follow them in wide movable range from opening to clenching. MAF is constructed with three discrete joint units, so that they are connected adapting to various pitch of operator's finger joints (Fig. 27). To make MAF narrow and short enough, each unit is designed possibly thin and aligned with partly overlapping. In this instance, all joints are coupled-driven by one relatively large motor (Faulhaber, model 1724SR).

As shown in Fig. 28, the actual rack is placed in opposite side viewed from the axis in comparison with the previous illustrations. The reason is to dissolve the interference between the mechanism and operator's finger that has came up in the previous arrangements. Inverse gear is added to correct the stretching direction of each segment and carried on a slider to keep the position at midpoint of the rack and the sector gear.



Fig. 26 Master finger mechanism (MAF) following various finger flexions.

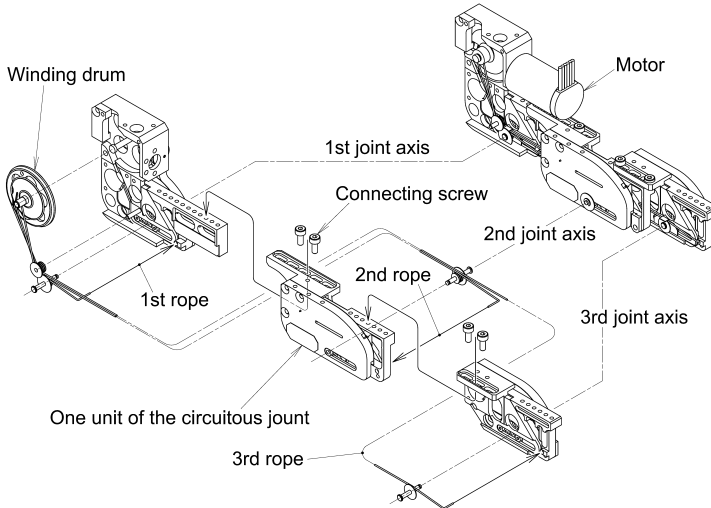


Fig. 27 Adjustable tandem connection of three joint units.

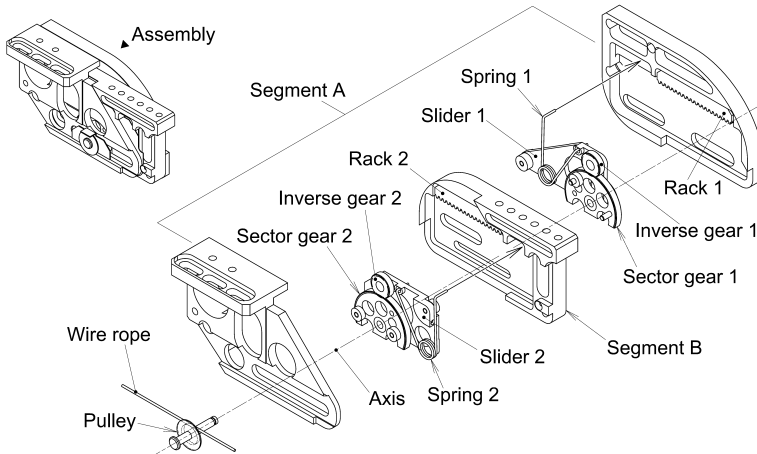


Fig. 28 Internal mechanism of the joint unit.

3.6 Master-Slave Control with Encounter-Type Force Feedback

As an ideal scheme of force display to the operator, the “encounter-type” has been proposed (McNeely, 1993, Tachi et al., 1994); that means a small object held up by a robot arm is approached and pressed to a part of operator’s body where tactile sensation is necessary as occasion demands. Its chief advantages are making the operator to discriminate clearly the two phases “non-contact” and “contact”, and free from constriction feeling during the non-contact phase. As it is suitable for the feature of my desired master hand, MAF introduced a function of non-contact following to the operator’s finger.

Since the present MAF has only 1DOF, the target motion of operator’s finger is reduced to same 1DOF, and a gap between both fingertips of MAF and the operator is set as the controlled variable during the non-contact phase. Concretely, a sensor at fingertip of MAF measures the gap, and MAF is position-controlled to keep the gap at the desired value 2mm.

Fig. 29 shows the fingertip assembly that contains a micro optical displacement sensor (Sanyo Electric, SPI-315-34), technically that detects motion of a swing reflector moved by the operator’s nail in slight force, and the gap is presumed from the motion.

During the contact phase, on the other hand, MAF should generate a desired contacting force against the operator’s fingertips at the contact tip of the fingertip assembly. So a film-like force sensor (Nitta, FlexiForce) on the contact tip measures the contacting force, and MAF is force-controlled by changing the motor torque of winding the rope in proportion to the difference between the measured and desired contacting forces.

An experimental master-slave system between MAF and a slave humanoid robot finger (SLF hereafter) was constructed as follows. SLF is always position-controlled to realize the same motion of MAF. The two phases of contact/on-contact on controlling MAF are switched according to detecting existence/non-existence of the contacting force on SLF. A film-like force sensor on the surface of SLF’s fingertip measures the contacting force, and the desired contacting force that MAF should generate is given as equal to that of SLF.

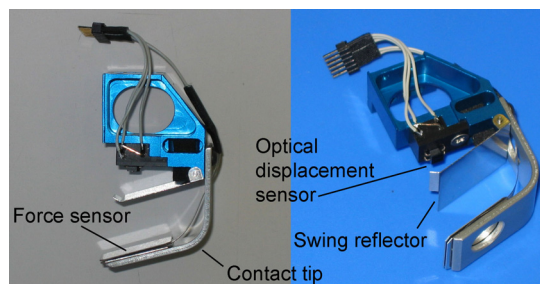


Fig. 29 Fingertip assembly for the master finger mechanism (MAF).

In order to confirm practicability of the master-slave system, an experiment was conducted. Fig. 30 shows the coupled motion of MAF and SLF in the non-contact phase; MAF was following the operator’s finger with keeping a small gap at the fingertips. MAF and SLF could follow the operator’s finger exactly as high as a less drastic speed. Since MAF had only 1DOF, SLF was prepared as the 1DOF mechanism interlocked all three joints. Moreover, the operator should also make his/her finger motion interlocking the three joints roughly similar to the behaviour of MAF. Though, I could forget an uncomfortable feeling by the fixed behaviour after familiarization, and enjoyed this experience.

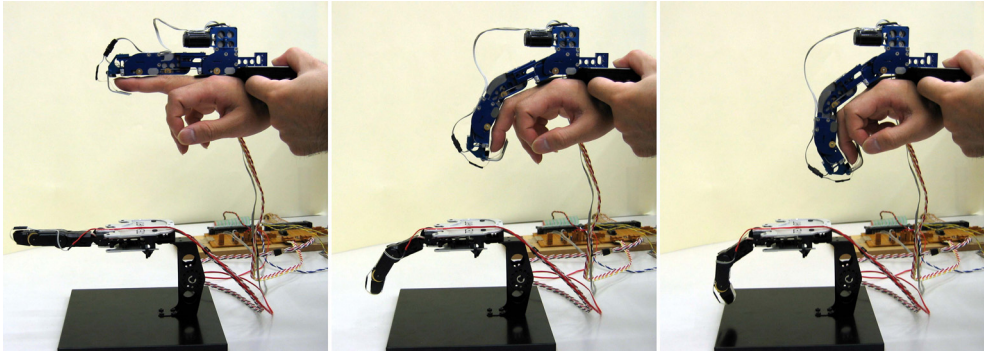


Fig. 30 Circumstance of the experimental master-slave control.

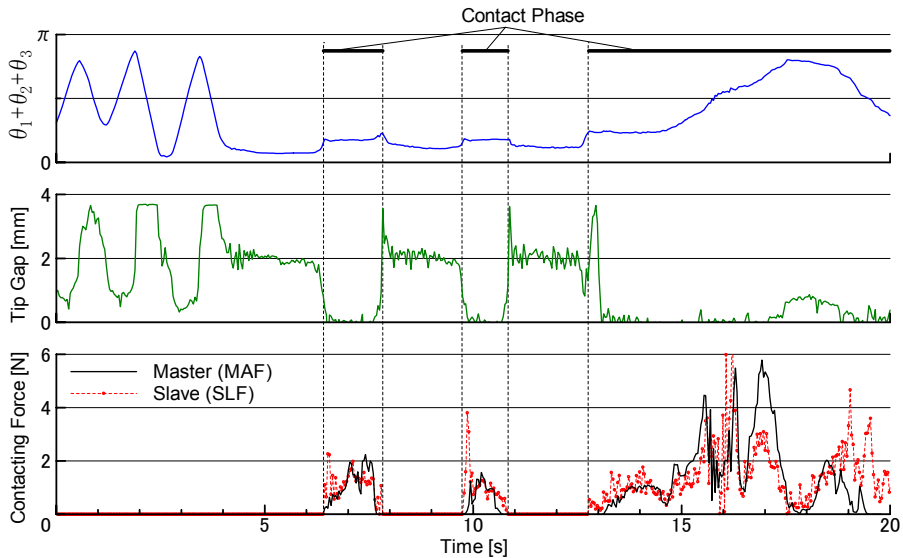


Fig. 31 Experimental result of transferring the contacting force.

Fig. 31 shows an experimental result; $\theta_1 + \theta_2 + \theta_3$ means the sum of three joint angular displacements on MAF. The two vital features are shown: prompt switching of contact/non-contact phases, and transferring the contacting force from SLF to MAF. The contacting force at the fingertip of SLF was given by an assistant pushing on it; for example, the two contact phases at the time 7s and 10s were caused by assistant's tapping. While the algorithm switching the phases was a primitive bang-bang control, an oscillation iterating contact/non-contact did not occur. I guess the reason: since the gap between the fingertips is kept small during the non-contact phase, the impact at the encounter that will lead the oscillation is not so serious, moreover the human fingertip has effective damping to absorb it. As shown by the curves after the time was 13s, the operator's finger could be moved by the assistant's force; the master-slave (bilateral) control with force feedback was verified. In conclusion of this experiment, MSF has enough performance as a principal part of the master hand for the Telexistence/Telepresence.

3.7 Overall view of the Master Hand

Since it comes to the end of width of this paper, I describe briefly the overall view of the master hand. By the way, the nomenclature of each joint is same as shown in the Fig. 1.

I gave four fingers to the master hand (Fig. 32); the little finger was omitted due to its little worth in general activities. The three finger mechanisms are same as shown in the Fig. 26, and the second and fourth finger have the abduction-adduction motion with active joints at $J_{2,1}$ and $J_{4,1}$. The each joint is position-controlled to follow lateral motion of the operator's finger detected at fingertip with similar sensor mechanism as shown in the Fig. 29; however, the additional sensor put beside the fingertip is omitted in the Fig. 32.

In the thumb mechanism, the distal three segments are constructed with two circuitous joints at $J_{1,4}$ and $J_{1,5}$. At the same time, elated ingenuity is exercised to design the joint mechanism corresponding to the carpo-metacarpal (CM) joint of operator; to make the two joint axes $J_{1,1}$ and $J_{1,2}$ intersected in an empty space for containing the CM joint, a slider mechanism is introduced where a motor-driven carriage runs on a sector rail in a wide circle. While the two joint axes $J_{1,3}$ and $J_{1,4}$ for the MP joint are not intersected, the order of each direction of joint axis and fingertip is identical to that of the Shadow hand (Fig. 2).

In the non-contact phase, the thumb mechanism is position-controlled to follow the operator's thumb opposing on both fingertips; each independent DOF has individual sensor similar to the previous one. As the mechanism does not touch the operator's thumb, slight deviation of the controlling is negligible. In the contact phase, only the joints $J_{1,4}$ and $J_{1,5}$ are switched its control mode to the force-control. More sophisticated control algorithm for this thumb mechanism is under study in the "Tachi S. laboratory in the university of Tokyo" where I started developing this master hand as a researcher in 2001.

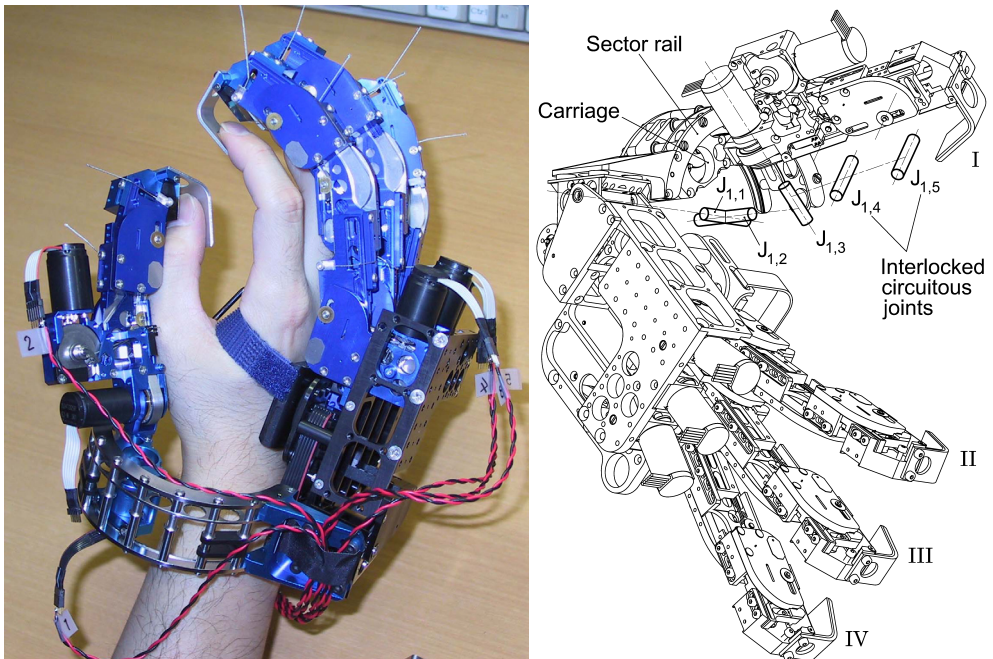


Fig. 32 Whole picture of the master hand.

4. Conclusion

To contribute on the evaluative process of searching the appropriate designing paradigms as a mechanical engineer, I bring up in this paper some of my ideas about the robot hand design concretely. While the designs of my robot hands may seem to be filled with eccentric, vagarious and serendipitous ideas for some people, I believe they are practical outcomes of flexible ingenuity in mechanical designing, so that they can take on pre-programmed but robust actuating roles for helping the programmable but limited actuators, and realize higher total balance in mechatronics. At the same time, for examining their practicability, reasonability and inevitability through the eyes of many persons, it will need to establish a standard definition and evaluation items in kinematics, dynamics, control algorithms and so on, that can subsume almost all humanoid robots. Concretely, a standard formats would be prepared to sort and identify any robot system by filling it. The Fig. 1 and 2 show my small trial of comprehensive comparison under a standard definition in the robot hand kinematics. And I hope the worldwide collaboration, so that it will promote developments of many sophisticated mechanical and electric elements that are easy to be used by many engineers like me who want any help to concentrate on his/her special fields.

5. Reference

- CyberGrasp: Immersion Co.
http://www.immersion.com/3d/products/cyber_grasp.php
- DLR Hand: German Aerospace Center
<http://www.dlr.de/rm/en/desktopdefault.aspx/tabid-398/>
- Gifu Hand: Dainichi Co., Ltd.
<http://www.kk-dainichi.co.jp/e/gifuhand.html>
- Harada Hand: Harada Electric Industry Inc.
http://www.h-e-i.co.jp/Products/e_m_g/ph_sh_2_004.html
- Jacobsen, S.C. et al. (1984). The UTAH/M.I.T Dextrous Hand: Works in Progress, *Int. J. of Robotics Research*, Vol.3, No.4 (1984), pp.21-50
- Lovchik, C.S. & Diftler, M.A.(1999). The Robonaut Hand: A Dexterous Robot Hand For Space, *Proc. of IEEE Int. Conf. on Robots & Automation*, Detroit, MI, May 1999
- McNeely, W.A. (1993). Robotic Graphics: A New Approach to Force Feedback for Virtual Reality, *Proc. of IEEE Virtual Reality Annual Int. Symp.*, pp.336-341, Seattle, Sep 1993
- NASA Hand: National Aeronautics and Space Administration
<http://robonaut.jsc.nasa.gov/hands.htm>
- Shadow Hand: Shadow Robot Company Ltd.
<http://www.shadowrobot.com/hand/>
- Tachi, S. et al. (1994). A Construction Method of Virtual Haptic Space, *Proc. of the 4th Int. Conf. on Artificial Reality and Telexistence (ICAT '94)*, pp. 131-138, Tokyo, Jul 1994
- Teleistence: Tachi, S. et al., Tele-existence (I): Design and evaluation of a visual display with sensation of presence, *Proc. of the RoManSy '84*, pp. 245-254, Udine, Italy, Jun 1984
- Telepresence: Minsky, M., TELEPRESENCE, *OMNI*, pp. 44-52, Jun 1980
- Weghel, M.V. et al. (2004). The ACT Hand : Design of the Skeletal Structure, *Proc. of IEEE Int. Conf. on Robots & Automation*, pp. 3375-3379, New Orleans, LA, Apr 2004